

Improved capacity spectrum method with inelastic displacement ratio considering higher mode effects

Sang Whan Han^{1a}, Sung Jin Ha^{*1}, Ki Hoon Moon^{1b} and Myoungsu Shin^{2c}

¹Department of Architectural Engineering, Hanyang University, Seoul 133-791, Republic of Korea

²School of Urban and Environmental Engineering, UNIST, Ulsan 689-798, Republic of Korea

(Received March 16, 2013, Revised March 5, 2014, Accepted March 9, 2014)

Abstract. Progressive collapse, which is referred to as the collapse of the entire building under local damages, is a common failure mode happened by earthquakes. The collapse process highly depends on the whole structural system. Since, asymmetry of the building plan leads to the local damage concentration; it may intensify the progressive collapse mechanism of asymmetric buildings. In this research the progressive collapse of regular and irregular 6-story RC ordinary moment resisting frame buildings are studied in the presence of the earthquake loads. Collapse process and collapse propagation are investigated using nonlinear time history analyses (NLTHA) in buildings with 5%, 15% and 25% mass asymmetry with respect to the number of collapsed hinges and story drifts criteria. Results show that increasing the value of mass eccentricity makes the asymmetric buildings become unstable earlier and in the early stages with lower number of the collapsed hinges. So, with increasing the mass eccentricity in building, instability and collapse of the entire building occurs earlier, with lower potential of the progressive collapse. It is also demonstrated that with increasing the mass asymmetry the decreasing trend of the number of collapsed beam and column hinges is approximately similar to the decreasing trend in the average story drifts of the mass centers and stiff edges. So, as an alternative to a much difficult-to-calculate local response parameter of the number of collapsed hinges, the story drift, as a global response parameter, measures the potential of progressive collapse more easily.

Keywords: capacity spectrum method (CSM); inelastic displacement; demand spectrum; higher mode; steel moment frame

1. Introduction

For conducting seismic performance evaluation of structures, it is important to estimate accurate inelastic seismic demands. Nonlinear response history analysis (RHA) is the most accurate procedure for estimating seismic demand, but nonlinear RHA requires intensive computational efforts, detailed knowledge of inelastic dynamic analysis and modeling (Krawinkler and Seneviratna 1998). Modeling and conducting nonlinear RHA may be a big burden to

*Corresponding author, Ph.D. candidate, E-mail: ha_sz@hotmail.com

^aProfessor, E-mail: swhan82@gmail.com

^bPost-Doc., E-mail: attr@hanmail.com

^cAssociate Professor, E-mail: msshin2020@gmail.com

practicing engineers. Many simple methods have been developed, which estimate the inelastic seismic demand using an approximate procedures (Ayala *et al.* 2012, Bento *et al.* 2010). Two methods have been widely used: (1) displacement coefficient method (FEMA356 2000), and (2) capacity spectrum method (ATC-40 1996).

The CSM was developed by Freeman (1978), in which inelastic displacement demand is obtained using capacity spectrum and demand spectrum. This method was adopted by ATC-40. The CSM specified in ATC-40 is called “ATC-40 CSM” hereafter. Inelastic pushover analysis is conducted for constructing capacity spectrum with a predetermined inertial force profile. From this analysis, the pushover curve is constructed, relating base shear force and roof drift. Then, by transforming base shear and roof drift into pseudo spectral acceleration (A) and into spectral displacement (D), capacity spectrum is obtained. Demand spectrum represents seismic demands (D and A) for various single degree of freedom (SDF) systems having different natural periods and damping ratios. In the CSM, the proper intersection point (D , A) between capacity and demand spectrums is determined using an iterative procedure in which demand curve is calibrated with effective damping ratios. Effective damping represents hysteretic damping plus viscous damping inherent in structures. The final spectral values (D , A) are then transformed to base shear and roof drift using transformation equations specified in ATC-40. The advantageous feature of the ATC-40 CSM is that it is able to predict inelastic displacement demand by using only static pushover analysis and repeated elastic response history analyses of SDF systems, without conducting nonlinear RHA.

Krawinkler (1995), however, pointed out that no physical principle exists that justifies the existence of a stable relationship between the hysteretic energy dissipation of the maximum excursion and equivalent viscous damping, particularly for highly inelastic systems. Fajfar (1999) reported that the period associated with the intersection of the capacity curve with the highly damped demand spectrum may have little to do with the dynamic response of the inelastic system. Chopra and Goel (1999) have reported that the ATC-40 CSM significantly underestimates the inelastic deformation demands for a wide range of structural periods with errors approaching 50%.

Fajfar (1999) and Chopra and Goel (1999) proposed the improved CSMs using a $R-\mu-T$ relationship instead of using equivalent viscous damping ratios for calibrating elastic demand spectrum in the CSM, where R is the strength reduction factor, μ is the ductility factor, and T is the natural period. In particular, the improved CSMs proposed by Fajfar (1999), and Chopra and Goel (1999) are named as the “N2 method” and the “capacity-demand-diagram method”, respectively. Aschheim and Black (2000) also proposed an improved CSM called the yield point spectra. This method used yield displacement. In the newly developed CSMs, inelastic displacement demand is determined by using the $R-\mu-T$ relationship without iteration, which is different from the ATC-40 CSM.

Miranda (2001) reported that the inelastic displacement obtained using the $R-\mu-T$ relationship is smaller than actual inelastic displacement demand. Using C_R , inelastic displacement demand is readily calculated by multiplying elastic displacement demand by C_R . Several researchers (Miranda 2001, Chopra and Chintanapakdee 2004) proposed equations that calculate the inelastic displacement ratio, C_R for bilinear SDF systems. However, C_R equations for bilinear SDF systems having a long period (say $T_n > 0.5$ sec) have been enforced by the equal displacement rule ($C_R = 1$), which leads to overestimating inelastic displacement. To avoid error in estimating inelastic displacement caused by using $R-\mu-T$ relation and equal displacement rule, this study proposed a new equation of C_R for bilinear SDF systems. Recently, FEMA440 (2005) proposed an improved procedure about the previous two methods. For displacement coefficient method, the

coefficients used in the procedure were more subdivide. And for capacity spectrum method, FEMA440 (2005) presented new expressions to determine effective period and effective damping.

Furthermore, the CSM produces inaccurate results for multi-degree-of-freedom (MDF) systems having significantly higher mode contribution. An adaptive pushover analysis has been developed to account for higher mode contributions in which the time variant distribution of inertial forces are used (Bracci *et al.* 1997, Gupta B and Kunnath 2000). Goel and Chopra (2004) pointed out that even if the adaptive pushover analysis gave better estimates of seismic demand than existing CSMs using a time invariant distribution of inertial forces, the analysis is overly conceptually complicated and too computationally demanding for routine application in structural engineering practice.

In response to this, Goel and Chopra (2004) developed a modal pushover analysis (MPA), which explicitly takes into consideration high mode contributions. In the MPA, modal pushover curves for the first significant modes are constructed by a pushover analysis using the invariant inertial force distribution of each mode. Using the hysteretic properties extracted from the modal pushover curve and structural dynamic properties for each mode, equivalent single degree of freedom system is constructed. By conducting nonlinear RHA for equivalent SDF systems subjected to ground motions, modal seismic demand is estimated. Then, by combining these modal seismic demands provides an estimate of the total seismic demand on inelastic system. Han and Chopra (2006) reported that MPA accurately predicts the seismic demand of steel moment frames using three modes under severe ground motions. Prasanth *et al.* (2008) applied MPA to estimate hysteretic energy demand.

This study proposed a CSM that does not even require nonlinear response history analyses of single degree of freedom systems, or a repeated linear response history analysis. The improved CSM can account for higher mode contributions. The modal combination concept of the MPA is very conveniently applicable in the format of the proposed CSM. To verify the accuracy of this proposed method, SAC LA and Seattle 3, 9 and 20-story moment frames (Gupta A and Krawinkler 1999) were tested. Ground motions for this study were taken from SAC LA and Seattle ground motions for 10/50 and 2/50 hazard levels (Somerville *et al.* 1997).

2. Improved CSM using inelastic displacement ration

Under horizontal ground motion, $\ddot{u}_g(t)$, the governing equation of motions for symmetric-plan buildings, is

$$\mathbf{m}\ddot{\mathbf{u}} + \mathbf{c}\dot{\mathbf{u}} + \mathbf{f}_s(\mathbf{u}, \text{sign}\dot{\mathbf{u}}) = -\mathbf{m}\boldsymbol{\iota}\ddot{u}_g(t) \quad (1)$$

where \mathbf{u} is the vector of N lateral floor displacements relative to the ground; \mathbf{m} and \mathbf{c} are the mass and damping matrices; and $\mathbf{f}_s(\mathbf{u}, \text{sign}\dot{\mathbf{u}})$ represents the nonlinear hysteretic relation between lateral forces and displacements. Each element of the influence vector $\boldsymbol{\iota}$ is equal to unity. Nonlinear response history analysis (RHA) can be used to solve above coupled equation by which seismic response is estimated as a function of time. In this study, the results obtained from nonlinear RHA are treated as exact estimates. Since nonlinear RHA requires excessive computation to estimate seismic response, this study develops an approximate procedure based on capacity spectrum method and modal pushover analysis using inelastic displacement ratio, C_R .

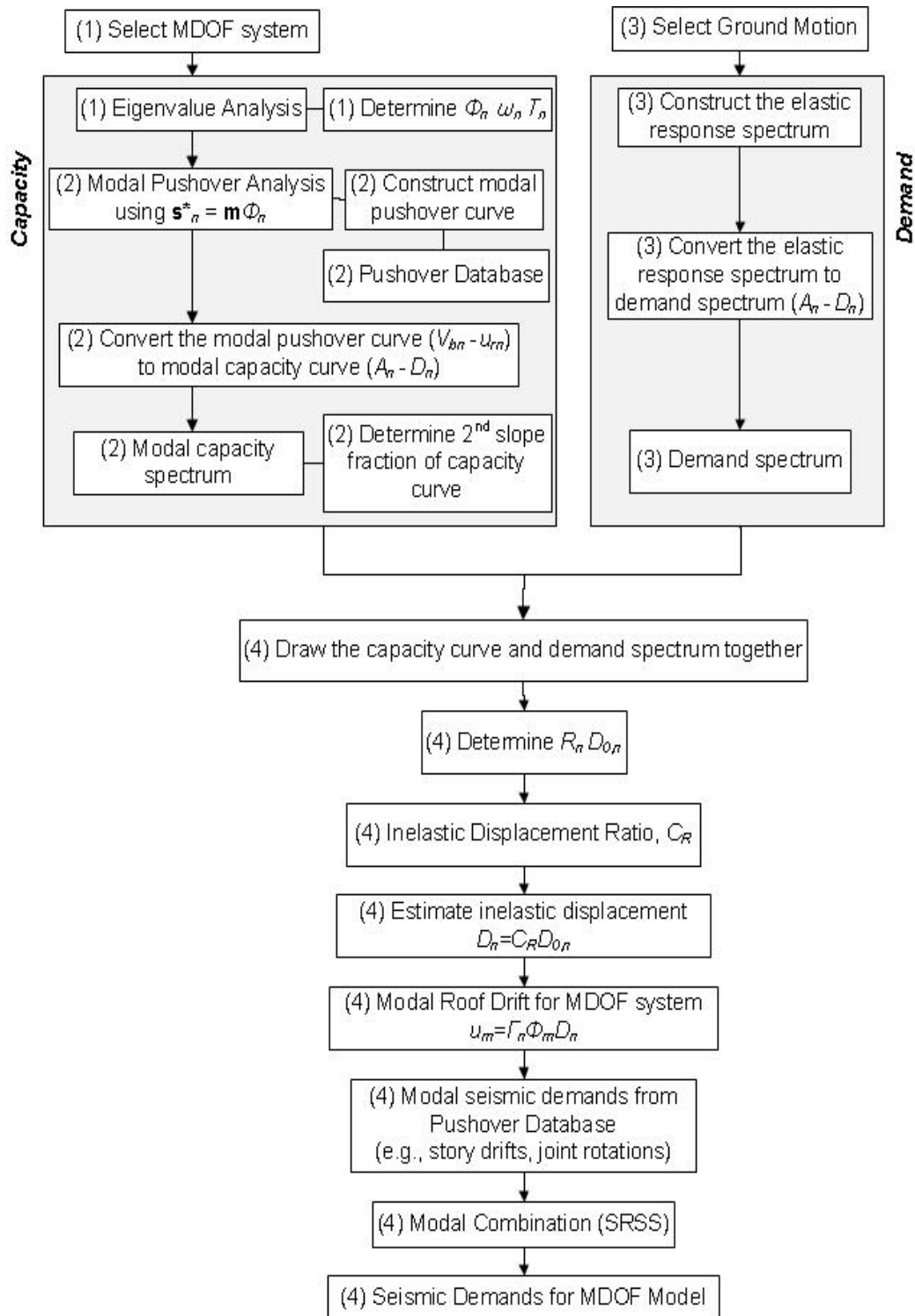


Fig. 1 Flow chart for the proposed CSM

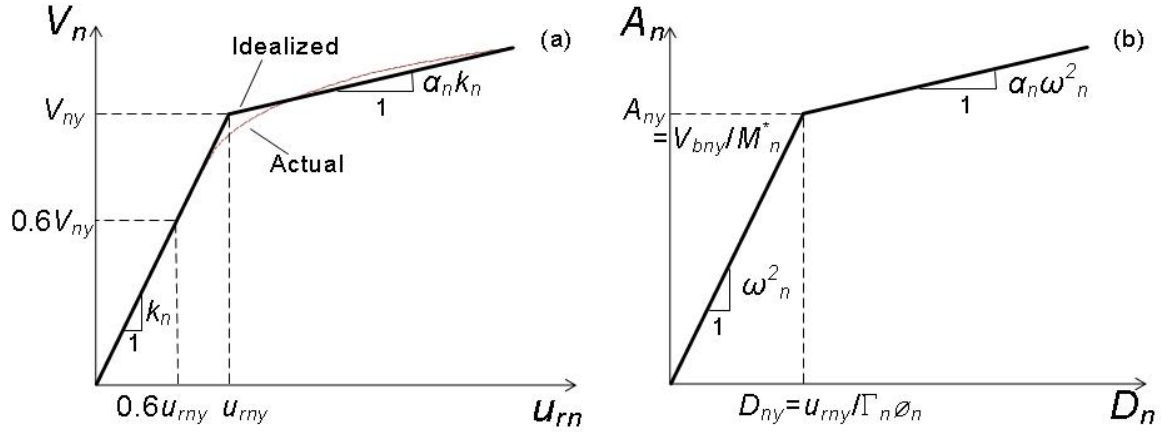


Fig. 2 Modal pushover curve (a) and modal capacity curve (b)

Fig. 1 shows the overall procedure for estimating seismic demand using the proposed CSM. The detailed explanation for each step is as follows.

(1) Select MDF frames

First, a model frame is selected, and the elastic dynamic properties of the frame are determined, such as periods of first significant modes, corresponding mode shapes, and damping ratios.

(2) Construct the modal capacity spectrum

The effective earthquake forces in Eq. (1) can be expanded into their modal components.

$$p_{eff}(t) = -m\ddot{u}_g(t) \tag{2}$$

This height-wise distribution of the effective earthquake forces on the building is defined by the vector $s \equiv m\boldsymbol{\iota}$ and $\ddot{u}_g(t)$. This force distribution can be expanded as a summation of modal inertia force distributions, s_n (Goel and Chopra 2004):

$$s = \sum_{n=1}^N s_n \quad s_n \equiv \Gamma_n m \boldsymbol{\phi}_n \tag{3a}$$

$$\Gamma_n = L_n / M_n = \boldsymbol{\phi}_n^T m \boldsymbol{\iota} / \boldsymbol{\phi}_n^T m \boldsymbol{\phi}_n \tag{3b}$$

where $\boldsymbol{\phi}_n$ is the n^{th} -mode shape vector. Note that subscript ‘ n ’ denotes the n^{th} mode. The effective earthquake force for the n^{th} mode, $p_{eff,n}(t)$, is:

$$p_{eff,n}(t) = -s_n \ddot{u}_g(t) \tag{4}$$

Next, a nonlinear static pushover analysis using the modal force distribution $s_n^* = m \boldsymbol{\phi}_n$ (based on Eq. (3b)) is conducted to construct the pushover curve, called the “modal pushover curve,” which represents the relationship between base shear force (V_n) and roof drift (u_{rn}). At each

loading step of the modal pushover analysis, response estimates, such as roof drift, story drift, floor displacement and joint rotation, are recorded in the database. This database will be used in the later step of this procedure (Chopra and Goel 2002).

The modal pushover curve is replaced with a bilinear curve from which lateral stiffness (k_n), 2nd slope (α_n), yield strength (V_{ny}), and yield displacement (u_{ny}) are estimated according to FEMA356. The lateral stiffness, k_n , is taken as the secant stiffness by connecting the origin to the point at a base shear force equal to 60% of V_{ny} . Fig. 2(a) shows the bilinear representation of the modal pushover curve. The modal pushover curve is then transformed to modal capacity spectrum using Eqs. (5) and (6). The modal capacity curve represents the relationship between the pseudo spectral acceleration (A_n) and spectral displacement (D_n) of an equivalent SDF system for the nth mode. Fig. 2(b) shows the modal capacity spectrum.

$$A_n = \frac{V_{bn}}{M_n^*} \quad (5)$$

$$D_n = \frac{u_{rn}}{\Gamma_n \phi_{rn}} \quad (6)$$

where $M_n^* = \Gamma_n L_n = (L_n)^2 / M_n$.

It is noted that the reversal pushover curve can be obtained when conducting the pushover analysis using higher mode force profile. Such is observed in very limited case. Chopra (2008) proposed two ways to treat the reversed pushover case. First, this issue is moot if the building does not deform beyond the elastic range during the ground motions considered in the mode with reversal in the pushover curve. This is indeed the case for the SAC-Los Angeles three-story building, which did not deform beyond the elastic limit in the third “mode” because of any of the ground motions in the 2/50 set developed for the SAC study, although these were very intense ground motions. Second, any “reversal” of the traditional pushover curve that plots base shear versus roof displacement may be eliminated if another floor displacement is used as the reference displacement. Energy based pushover analysis proposed by Hernandez-Montes *et al.* (2004) can solve such problem as well. Since the displacement of the 3rd mode rarely exceed the elastic limit and its contribution is relatively small, both methods can be reliably used. However, this phenomenon was not clearly considered in this manuscript.

(3) Construct demand curves

Demand spectrum is constructed in a domain of A_n and D_n by conducting linear RHA of SDF systems having various natural periods subjected to ground motions. For an ensemble of ground motions, median demand curves are constructed. The median estimate of pseudo spectral acceleration, A_n , is calculated using the following equation:

$$x_n = \exp \left[\left(\frac{\sum_{i=1}^N \ln x_{ni}}{N} \right) \right] \quad (7)$$

where $x_n = A_n$ and $x_{ni} = A_{ni}$. Note that A_{ni} is the pseudo spectral acceleration of the SDF system under the ith ground motion, N is the number of ground motions, ω_n is the natural circular

frequency of the n^{th} mode. Median spectral displacement, D_n , is estimated using Eq. (8).

$$D_n = A_n / \omega_n^2 \tag{8}$$

where A_n is the median pseudo spectral acceleration. This study observed that median spectral displacement D_n calculated using Eq. (8) coincides with that obtained using Eq. (7) ($x_n = D_n$, $x_{ni} = D_{ni}$), which is not presented in this paper. Design response spectrum in the current design provisions can be also used to construct the demand curve by using Eq. (8). Fig. 3 shows individual and median response spectrum of 20 ground motions.

(4) Determination of inelastic displacement demand

Capacity spectrum for the first significant modes (2-3 modes) and elastic demand spectrum are plotted together and shown in Fig. 4. Elastic displacement and force demand (D_n, A_n in Fig. 3) is determined by tracing the intersecting point of the elastic demand curve and a line extended from the elastic part of the modal capacity spectrum (denoted by the dotted line). Then, inelastic displacement demand is calculated by multiplying D_n by the inelastic displacement ratio, C_R . The inelastic displacement ratio, C_R is defined as a ratio of peak displacement ($D_{n-inelastic}$) of the inelastic SDF system to the peak displacement (D_n) of the corresponding elastic SDF system (Eq. (9)), which has the same mass, elastic stiffness and damping ratio (Fig. 5).

$$C_R = \frac{D_{n-inelastic}}{D_n} \tag{9}$$

Many researchers (Miranda 2004, Chopra and Chintanapakdee 2004, Ramirez *et al.* 2002) proposed C_R equations for bilinear SDF systems using regression analysis. In most C_R equations, the equal displacement rule (FEMA356 2000) was enforced ($C_R = 1$) for systems having long period range (say $T_n > 0.5$ sec). It is observed that the equal displacement rule overestimates displacement demand of bilinear SDF systems having a long period (Ramirez *et al.* 2002). To avoid such overestimation, this study proposed C_R equation for bilinear SDF systems having a damping ratio of 5% using the regression analysis, which is shown in Eq. (10a). Table 1 summarizes the coefficients for Eq. (9). In this study, Eqs. (10a)-(10b) were used for calculating inelastic displacement ratio for bilinear SDF systems.

$$C_R = a^{(R-1)^b} + \frac{c \cdot (R-1)^d}{T^e \cdot R^f \cdot [g + (100\alpha)^h]} \tag{10a}$$

$$R = \frac{A_n}{A_{ym}}, \quad T = 2\pi \sqrt{\frac{D_n}{A_n}} \tag{10b}$$

where α is the post yield stiffness. The detailed explanation how to construct C_R equation is given in the following section. For calculating C_R , R factor (the key component of C_R) has to be determined. As shown in Fig. 4, R factor is readily determined using the proposed CSM, which is

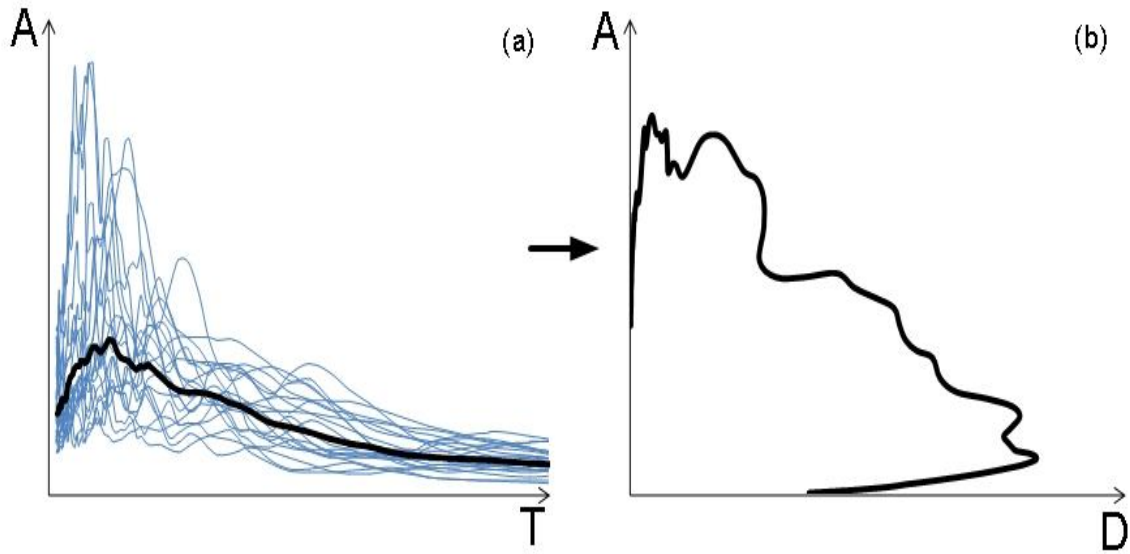


Fig. 3 Individual and median linear response spectrum and corresponding demand spectrum

Table 1 Coefficients of median C_R

	<i>a</i>	<i>b</i>	<i>c</i>	<i>d</i>	<i>e</i>	<i>f</i>	<i>g</i>	<i>h</i>
$T_n \leq 0.8$	1.00	0.50	0.34	2.82	2.19	2.76	3.12	0.75
$T_n > 0.8$	0.82	0.64	0.62	0.13	0.12	-0.65	4.85	0.50

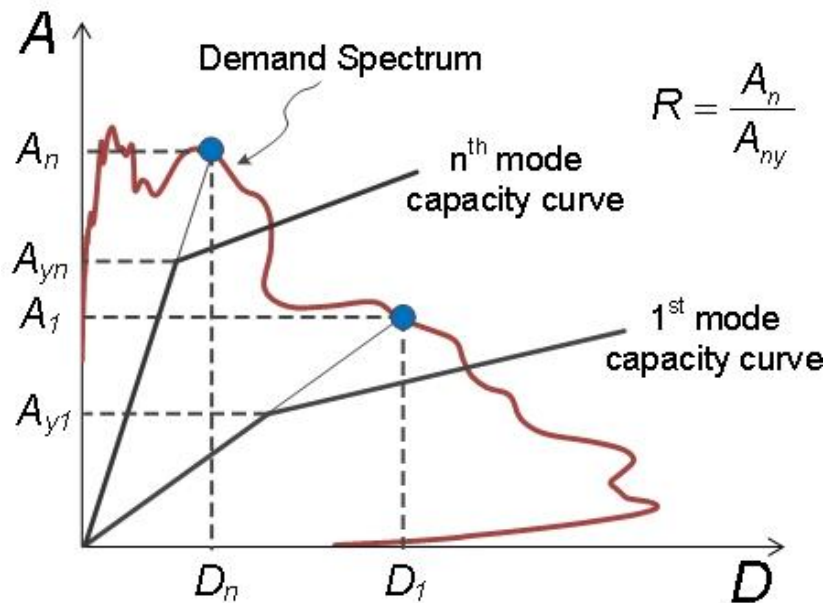


Fig. 4 Individual and median linear response spectrum and corresponding demand spectrum

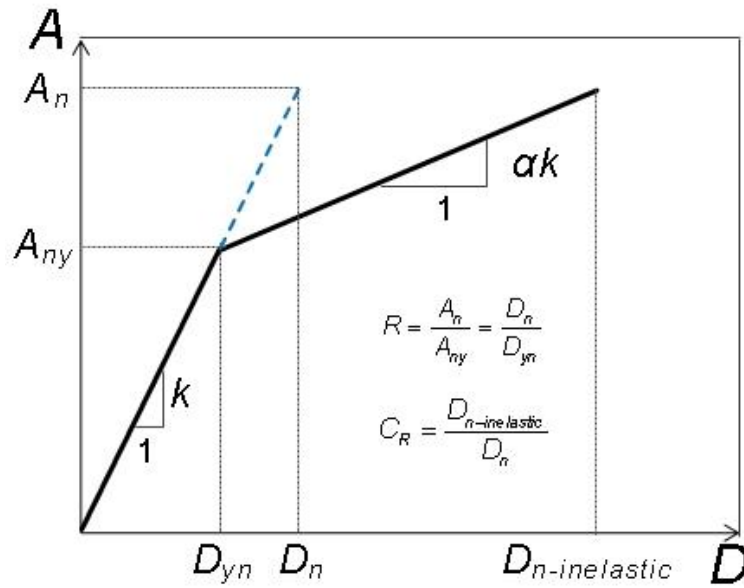


Fig. 5 Force displacement relationship in a bilinear system

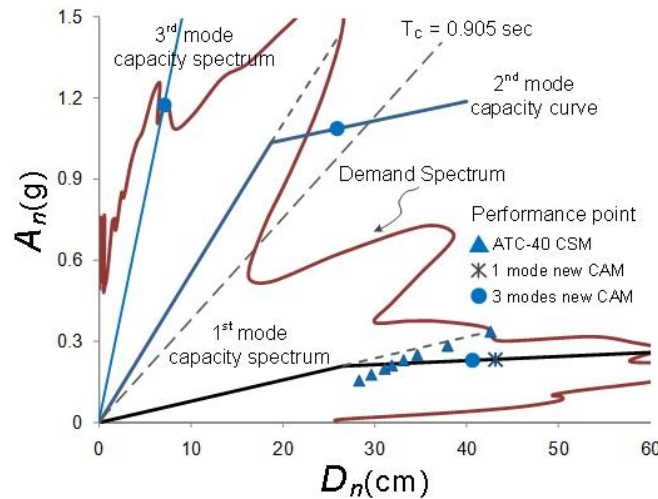


Fig. 6 Performance points for SAC LA 9 story building under LA 23 ground motion (PGA=0.418g)

another advantageous feature of the proposed CSM. After estimating inelastic displacement of bilinear SDF systems for the n^{th} mode ($=C_R \times D_n$), modal roof drift (u_m) is determined using following equation.

$$u_m = \Gamma_n \times \phi_m \times D_n \times C_R \tag{11}$$

For the calculated roof drift, u_m , other modal seismic response demands (r_n) can be readily determined from the database previously constructed during the pushover analysis. In this study

roof drift ratio and story drift ratio were considered as seismic response demand.

Fig. 6 shows seismic demands for SAC LA 9 story building obtained from different CSM methods under LA 23 ground motion (PGA=0.418g). For the ATC-40 CSM, starting from the intersecting point between the capacity and demand spectrums, inelastic displacement demand is determined using an iterative procedure in which demand spectrum is calibrated using equivalent damping ratios and equivalent period until the difference between i^{th} and $i+1^{\text{th}}$ inelastic displacement is less than a given tolerance level. For the N2 method, inelastic displacement is calculated by elastic yield displacement multiplied by a ductility factor, μ . In the proposed CSM, inelastic displacement demands for first significant 3 modes in Fig. 6 are estimated by multiplying elastic displacement demand by C_R .

To estimate median roof drift ratio and median story drift ratio, two procedures were considered. In the first procedure, the n^{th} mode median estimate of elastic response spectrum (D_n) is calculated using Eq. (7) with 20 individual estimates of elastic response spectrum (D_n). The n^{th} mode median inelastic displacement spectrum is then determined by C_R times D_n . The n^{th} mode roof drift (u_m) is then estimated using Eq. (6) with the n^{th} mode median inelastic displacement spectrum. The n^{th} mode story drifts corresponding to median u_m throughout the building were extracted from the database previously constructed from inelastic pushover analyses. Total seismic response demand (r) is then estimated using the SRSS modal combination rule (Eq. (12)).

$$r = \sum_{i=1}^n r_n^2 \quad (12)$$

In the 2nd procedure, the n^{th} mode individual (i^{th}) inelastic displacement spectrum for an ensemble of ground motions is estimated by multiplying D_{ni} by C_R . Corresponding to each n^{th} mode inelastic displacement, the n^{th} mode roof drift is determined using Eq. (11). For each n^{th} mode roof drift ratio, the n^{th} mode story drifts are determined from the database constructed during the modal pushover analysis. The n^{th} mode median story drift ratios are then estimated using Eq. (7). Total seismic response demand is then calculated using Eq. (12).

Fig. 7 shows the median story drift ratios of the SAC LA 20 story building obtained from 2 different procedures. Even though story drift ratios obtained from the 2 different procedures are not exactly the same, their differences are small. This study used the 1st procedure to estimate median story drift ratios since it is simpler to use.

3. Inelastic displacement ratios C_R

In this study, an equation of C_R for bilinear SDF systems was proposed using the statistical analysis. An ensemble of 60 ground motions were used as input ground motions: 20 ground motions recorded at each of three firm sites with site class B, C, and D classification (Bracci *et al.* 1997). These ground motions were recorded during earthquakes of magnitudes ranging from 6.0 to 7.4, at distances of 11 to 18 km. This study conducted 3,000 (=50×60) repeated linear response history analyses (RHA) and 312,000 (=50×13×8×60) repeated nonlinear RHA with combinations of the variables shown in Table 2.

Fig. 8 shows median inelastic displacement ratio with respect to post yield stiffness, α , and

natural period, T_n , obtained under 60 ground motions. In this figure, median C_R becomes smaller with increasing T_n . In particular, C_R sharply decreases with increasing T_n in the short period range. This study also observed that C_R becomes smaller with increasing α . Fig. 9 is another plot showing the influence of α and R on for bilinear SDF systems having natural periods of 0.2 and 1 second. As shown in Fig. 8, C_R decreases with increasing α . A more significant reduction in C_R is observed in short period systems (0.2 sec) having a small α (Figs. 9(a)-(b)).

In short period systems (0.2 sec), C_R becomes larger with increasing R (Fig. 9(a)), whereas in long period systems (1.0 sec), the effect of R on C_R is small (Fig. 9(b)). It is observed that the dependence of C_R on α is strong in short period systems (see Fig. 9(a)), whereas the influence of α on C_R in long period systems is weak (see Fig. 9(b)). The greatest value of C_R is obtained when $\alpha = 0$, irrespective of natural periods (Figs. 9(a)-(b)). For the long period system

(1 sec), C_R is smaller than 1, regardless of the values of α and R . These results indicate that the equal displacement rule overestimates the inelastic displacement in such systems.

To determine median C_R for bilinear SDF systems having 5% damping ratio, the regression analysis was conducted using 31,200 C_R calculated by repeated linear and nonlinear response history analyses. Eq. (13) is the same equation as Eq. (10), which is re-written for convenience. The coefficients used in Eq. (13) are summarized in Table 1. It is noted that Eq. (14) is the same equation with Eq. (9) and re-written for convenience.

$$C_R = a^{(R-1)^b} + \frac{c \cdot (R-1)^d}{T^e \cdot R^f \cdot [g + (100\alpha)^h]} \tag{13}$$

In Fig. 10, median C_R calculated using the proposed equation is compared with that obtained from nonlinear and linear response history analyses. The deviation (e) of C_R calculated using Eq. (13) from exact C_R is calculated using the following equation.

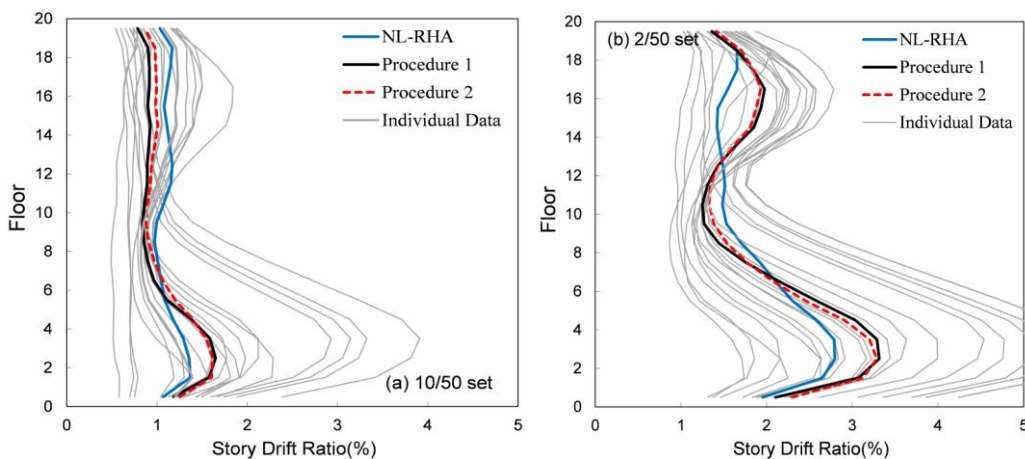


Fig. 7 Distributions of Story drift ratios obtained from two different procedures for SAC LA 20 story building: SAC LA 10/50 (a) and 2/50 ground motions (b)

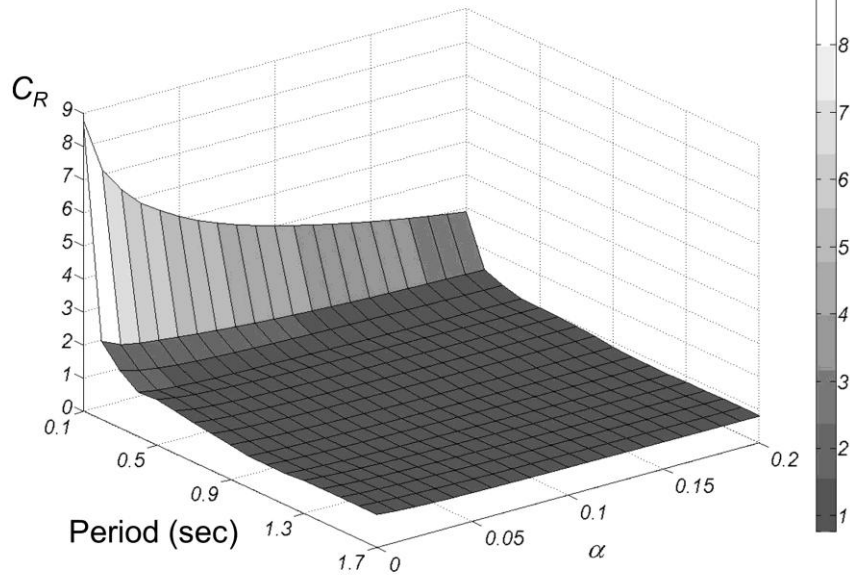


Fig. 8 Median C_R with respect to post yield stiffness α and natural period for $R = 4$

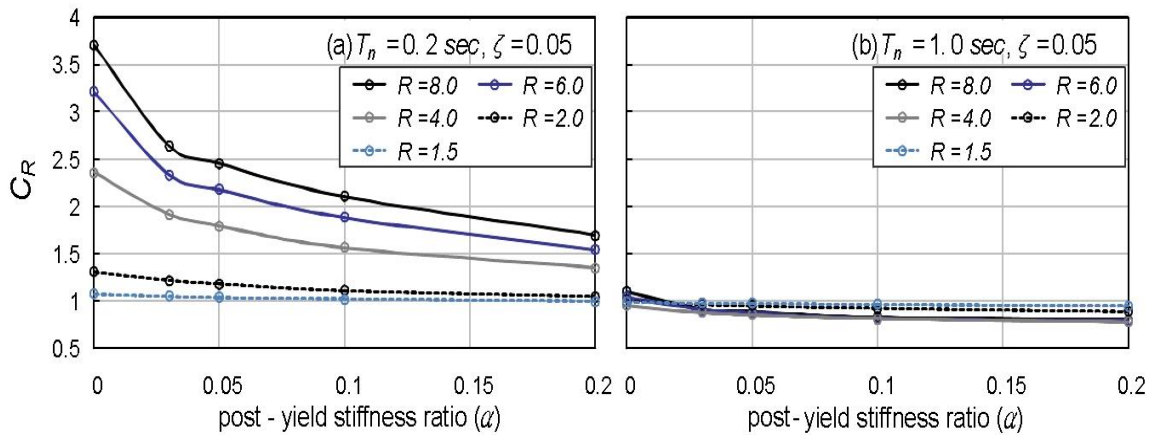


Fig. 9 Median C_R with respect to post yield stiffness α

Table 2 Variables for statistical studies for median C_R

Variable	Range	Number
T_n	0.1~5.0 ($\Delta T_n = 0.1$)	50
α	0~0.10 ($\Delta\alpha = 0.01$), 0.15, 0.20	13
R	1.5, 2~8 ($\Delta R = 1$)	8
Ground motions		60

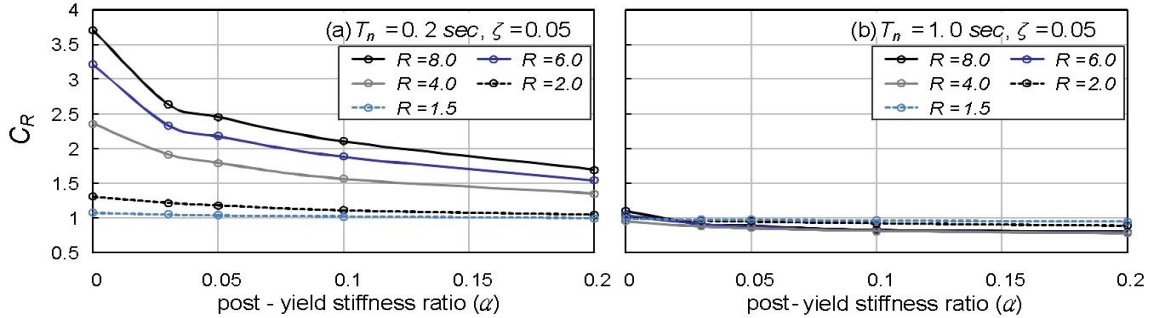


Fig. 9 Median C_R with respect to post yield stiffness α

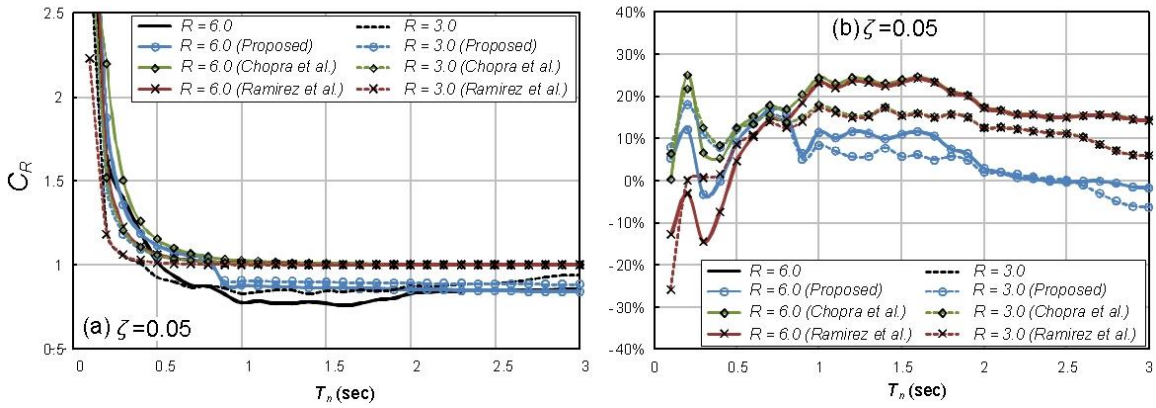


Fig. 10 Median C_R and errors in predicted C_R from actual median C_R

$$e(\%) = \frac{|x_{approximate} - x_{exact}|}{x_{exact}} \times 100 \quad (14)$$

Fig. 10 shows that the proposed equation predicts median C_R for bilinear SDF systems with good accuracy.

4. Verification of the proposed CSM

4.1 Model Frames and ground motions

This study considered SAC LA and Seattle 3, 9, and 20 story buildings (Gupta A and Krawinkler 1999) as model frames, shown in Fig. 11. The model frame was idealized by the M1 model, which is a basic centerline model (Gupta A and Krawinkler 1999). Plastic hinges at the beam (or column) ends in the frame were modeled by bilinear, kinematically hardening moment-rotation springs with post-yield stiffness equal to 3%. P- δ effects due to gravity loads were not considered in this study. The damping matrix in Eq. (1) was chosen as $\mathbf{c} = a_0 \mathbf{m} + a_1 \mathbf{k}$, where \mathbf{k} is

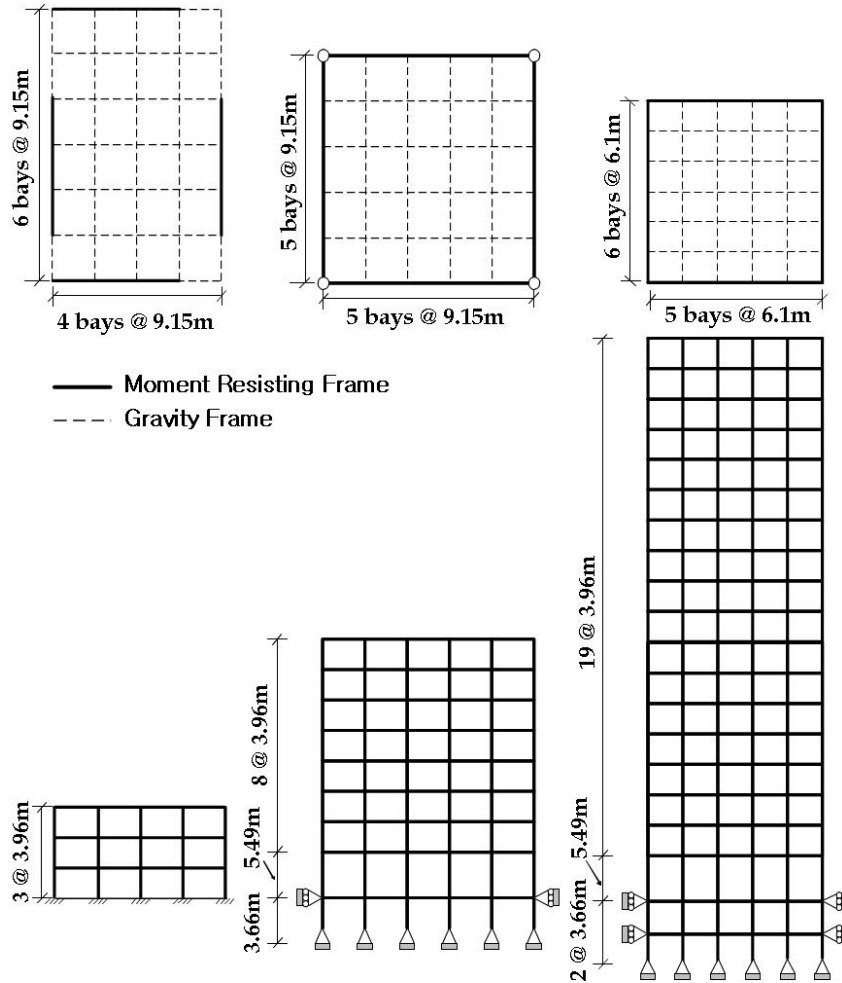


Fig. 11 Model frames (Gupta A and Krawinkler 1999)

determined from specified damping ratios at 2 periods. For 3- and 9-story buildings, damping ratios of 5% were specified at the first-mode period and at 0.2 sec. For the 20-story building, damping ratios of 5% were specified at the first and 5th-mode. According to FEMA356, the number of the modes included in the analysis shall be determined to contain effective modal mass greater than 90%. Two, three and four modes are considered for 3, 9, and 20story buildings; these buildings correspond to effective modal masses of 96.3%, 97.7%, and 95.1%, respectively. For the SAC Seattle 3-, 9-, and 20-story buildings, the consideration of 2, 3, and 4 modes corresponds to effective modal masses of 95.9%, 97.2%, and 97.1%, respectively. Table 3 summarizes natural periods, and post yield stiffness of the model frames.

SAC LA and Seattle 10/50 and 2/50 sets of ground motions were used for input ground motions (Somerville *et al.* 1997) for the SAC LA and Seattle buildings, respectively; 10/50 and

2/50 denote 10% and 2% exceedence probability in 50 years, respectively. For each ground hazard levels (10/50 and 2/50), an ensemble of 20 horizontal ground motions were used. These were recorded at sites classified into site class D according to NEHRP provisions (Gupta A and Krawinkler 1999).

In this study, the seismic demands obtained from the proposed method were compared with those obtained from nonlinear RHA, from the ATC-40 CSM, and from the N2 method. Software drain 2DX (Prakash *et al.* 1993) was used in conducting nonlinear RHA for the model buildings. Seismic demands estimated from nonlinear RHA were considered as exact estimates. For calculating inelastic displacement using the N2 method, the equations proposed by Nassar and Krawinkler (1991) of $R-\mu-T$ relationship for bilinear SDF systems were used. For the ATC-40 CSM and N2 methods, a pushover analysis was conducted under the height-wise distribution of an effective earthquake force for the 1st mode.

Figs. 12-13 show the distribution of story drift ratios throughout the building obtained from the different methods (nonlinear RHA, ATC-40 CSM, N2, and proposed CSM), and show the distribution of the ratio of story drifts from approximate methods to those from nonlinear RHA, which represents the deviation of approximate drift from exact drifts.

4.2 SAC Seattle buildings

The 3-story SAC Seattle building behaved within elastic range under SAC Seattle 10/50 ground motions. The first mode governs the dynamic response of the 3-story frame. No distinctive difference was found between story drift ratios calculated using the proposed CSM with considering either the 1 mode or the 2 modes (see Fig. 12(a) and (d)). For the 3-story building, all approximate methods (ATC-40 CSM, N2 and the proposed CSM) indicate similar story drift demands. The accuracy of the proposed method is slightly improved compared to ATC-40 CSM and N2 method.

For the 9-story SAC Seattle building under the 10/50 ground motions, the accuracy in predicting the story drift ratio was significantly improved by using the proposed CSM. All 3 approximate methods underestimated the story drift ratios (Fig. 12(b) and (e)). The largest underestimation using Eq. (14) was 22% at the 8th story for the proposed CSM whereas the largest underestimation for the ATC-40 CSM and N2 method was 62% at the 9th story.

For the 20 story SAC Seattle building, 3 approximate methods produced story drift ratios smaller than the exact story drift ratios. The largest underestimation of story drift ratio using the proposed CSM was 30% at the 18th floor, whereas it was 74% smaller than the exact estimate using the ATC-40 CSM, and N2 methods.

Under the SAC Seattle 2/50 ground motions, the ATC-40 CSM produced smaller story drift ratios than did the N2 method and the proposed CSM (see Fig. 12(g) and (i)). For the 3 story SAC Seattle building, the ATC-40 CSM underestimated the story drift demand, whereas the N2 and the proposed methods produced more accurate story drift ratios than the ATC-40 CSM.

For the 9 story building under the Seattle 2/50 ground motions, the ATC-40 CSM underestimated story drift demands throughout the building (Fig. 12(h) and (k)). The N2 method accurately predicted the story drift ratios in lower stories but underestimated story drift ratios in upper stories. The largest error in predicting story drift ratios using the N2 method is 67% at the 9th story. The underestimation resulting from the approximate methods was significantly reduced by using the proposed CSM up to 19%, which was detected at the 7th story.

Under the 2/50 ground motions, story drift ratios of the 20 story SAC Seattle building were

underestimated by the ATC-40 CSM, the N2 method, and the proposed CSM (Fig. 12(i) and (l)). The largest underestimation using the ATC-40 CSM and N2 method was 73% at the 18th story whereas the largest underestimation using the proposed CSM was 27% at the 17th story.

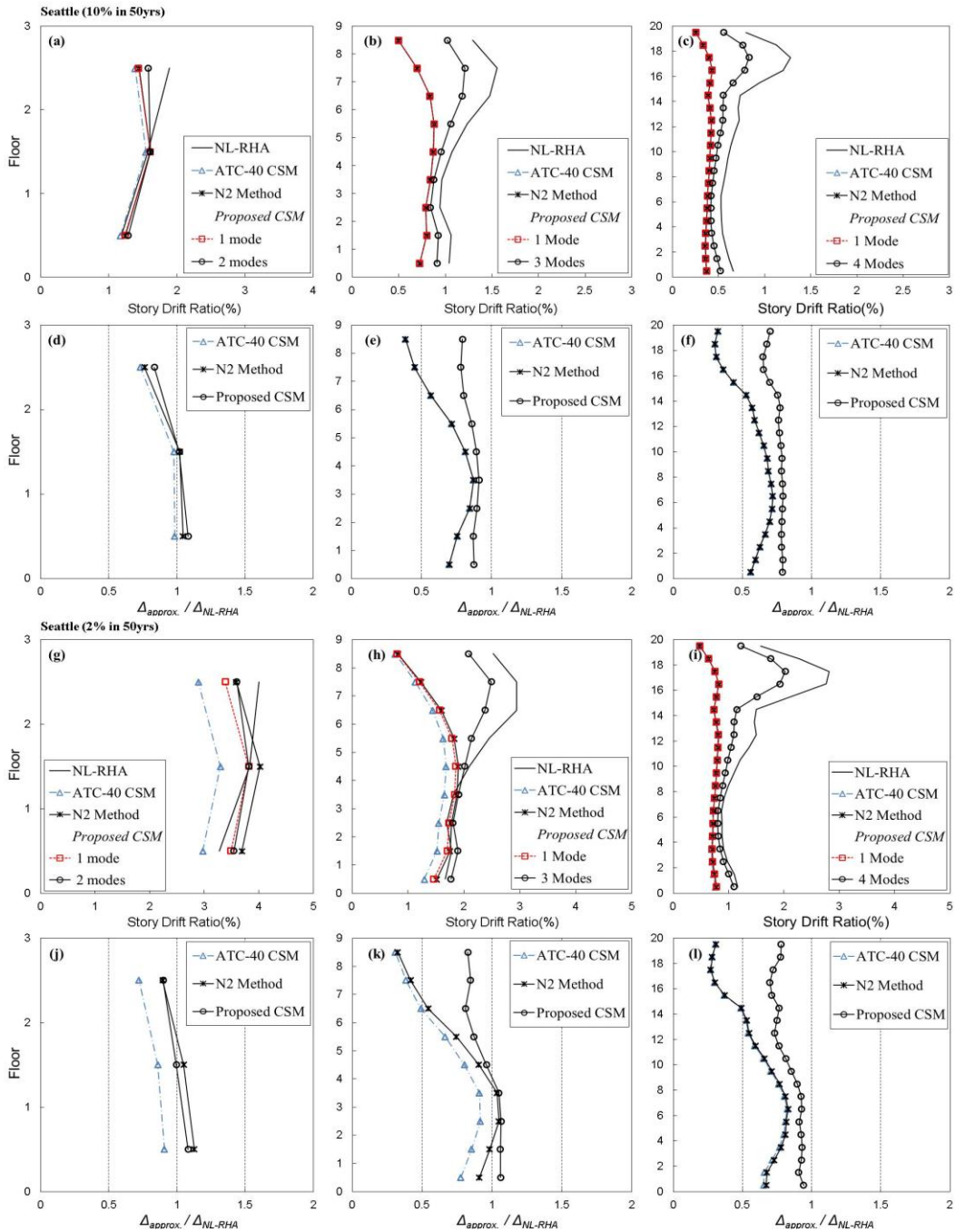


Fig. 12 Distribution of story drift ratio of SAC Seattle buildings under SAC Seattle ground motions

4.3 SAC LA buildings

For the 3 story SAC LA building, the proposed CSM and the N2 methods produced similar results since the building was mostly governed by the 1st mode, whereas the ATC-40 CSM produced smaller story drift ratios than the N2 method and the proposed CSM (Fig. 13(a)). Under 10/50 ground motions, the largest underestimation using the ATC-40 was 21% at the 3rd story, whereas the largest error was 10% at the 2nd story, this time in overestimation, using the N2 and the proposed CSM (Fig. 13(d)). Under 2/50 ground motions, all the 3 approximate methods provided similar story drift ratio; the largest underestimation was 15% at the 3rd story (Fig. 13(j)).

For the 9 story SAC LA building, under 10/50 ground motions, the largest error using the proposed method was 23% overestimation at the 2nd story. In upper stories, story drift ratios were, however, underestimated by the proposed CSM; the largest underestimation was 18% at the 8th story (Fig. 13(b) and (e)). The ATC 40-CSM underestimated the story drift ratios throughout the building, with the largest underestimation of 54% at the 9th story. The largest underestimation and overestimation using the N2 method were 23% at the 2nd story, and 52% at the 9th story, respectively. Under the 2/50 ground motions, similar observation is made. The largest underestimation and overestimation using the proposed method were 22% and 17% at the 9th and the 2nd stories, respectively. Those due to the N2 method were 53% at the 9th story and 25% at the 2nd story, respectively. The ATC-40 CSM underestimated story drift ratios throughout the building. The largest underestimation was 60% at the 9th story (Fig. 13(h) and (k)).

For the 20 story building under the 10/50 ground motions, the proposed CSM and N2 methods underestimated story drifts in upper stories, but they overestimated story drifts in lower stories. The proposed CSM produces the most accurate results in predicting story drifts among the 3 approximate methods; the largest overestimation using the proposed CSM was 25% at the 4th story. Under the 2/50 ground motions, the largest error (overestimation) resulting from the proposed CSM was overestimated by 35% at the 16th story, whereas the largest error (underestimation) using the ATC-40 CSM and N2 methods is underestimated by 65% (Fig. 13(i) and (l)).

Table 3 Properties of model frames

Building	Modal period (s)				Modal post-yield stiffness ratio			
	T_1	T_2	T_3	T_4	α_1	α_2	α_3	α_4
LA 3-story	1.01	0.33	-	-	0.04	0.02	-	-
LA 9-story	2.27	0.85	0.49	-	0.19	0.13	0.14	-
LA 20-story	3.81	1.32	0.77	0.54	0.07	0.06	0.03	0.03
Seattle 3-story	1.32	0.43	-	-	0.04	0.02	-	-
Seattle 9-story	2.99	1.08	0.59	-	0.05	0.04	0.05	-
Seattle 20-story	3.76	1.36	0.79	0.54	0.09	0.05	0.05	0.03

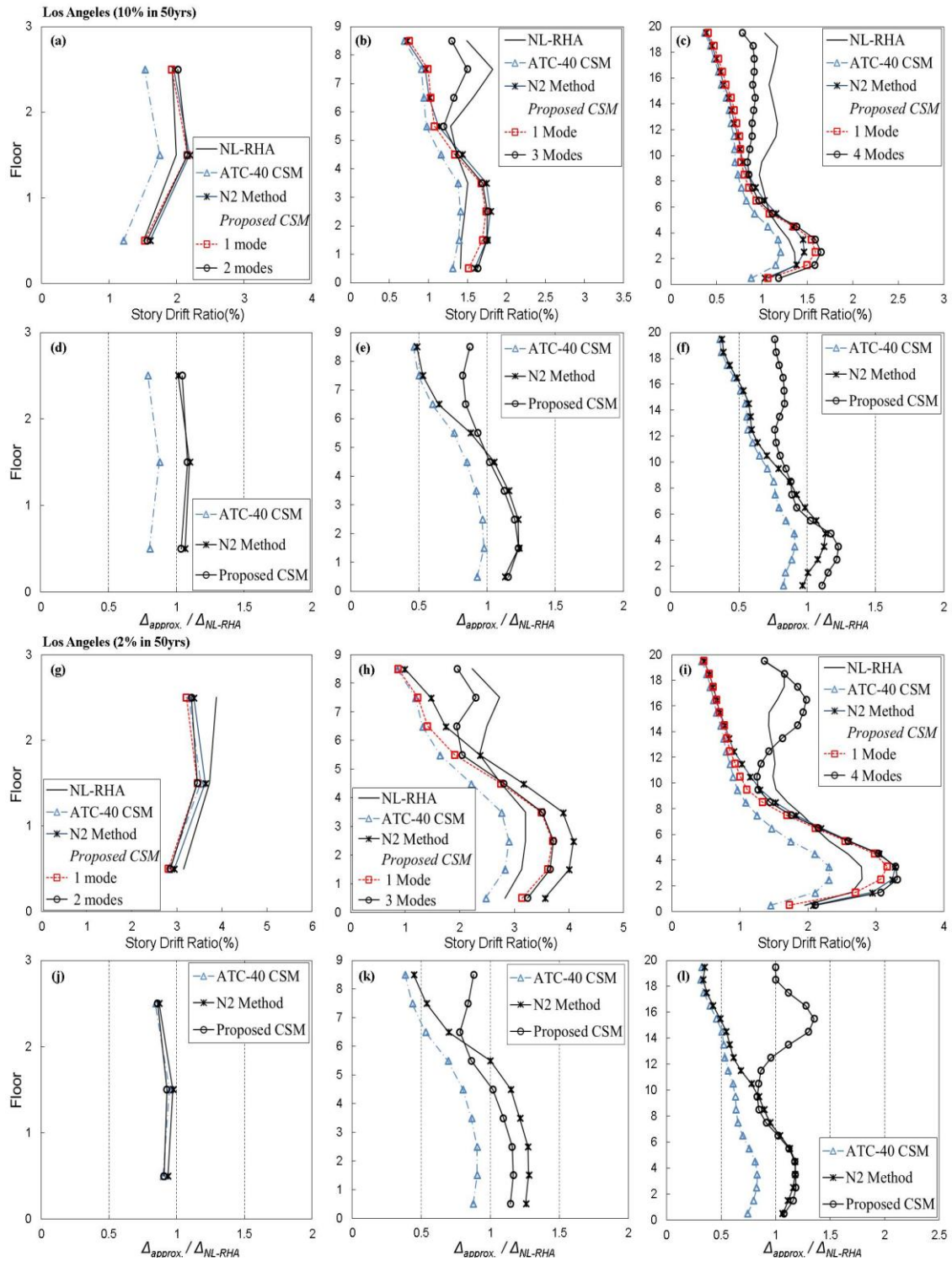


Fig. 13 Distribution of story drift ratio of SAC LA buildings under SAC LA ground motions

5. Conclusions

This study developed a CSM using the inelastic displacement ratio, C_R . Thus, using this new CSM, inelastic seismic demands can be accurately estimated using elastic demand spectrum and C_R . To avoid underestimation resulting from using the equal displacement rule for bilinear SDF systems, this study proposed an equation of median C_R for bilinear SDF systems with 5% damping ratio. Since this CSM adopts inelastic displacement ratio, no iteration is required to determine inelastic displacement demand (as is required by the ATC-40 CSM).

Furthermore, the proposed CSM is able to account for higher mode contributions of MDF systems by combining inelastic displacements of equivalent SDF systems for first four modes using a conventional modal combination rule. The modal combination can be very conveniently incorporated into the CSM using C_R and R . This study used 3-, 6-, and 9-story SAC LA and SAC Seattle buildings to verify the accuracy of this new CSM. SAC 10/50 and 2/50 ground motions were used as input ground motions. This study proved that the proposed CSM more accurately predicted median story drift ratios throughout the tested buildings than did the ATC-40 CSM and the N2 methods.

Acknowledgments

This work was supported by the National Research Foundation of Korea (NRF) grant funded by the Korea government (MSIP) (No. 2012R1A2A2A06045129).

References

- Aschheim, M. and Black, E.F. (2000), "Yield point spectra for seismic design and rehabilitation", *Earthq. Spectra*, **16**(2), 313-335.
- ATC (1996), "Seismic evaluation and retrofit of concrete buildings", *Appl. Tech. Council*, **40**, Redwood City, CA.
- ATC. (2005), "Improvement of nonlinear static seismic analysis procedures", FEMA 440 Federal Emergency Management Agency, Washington, DC.
- Ayala, A.G., Castellanos, H. and Lopez, S. (2012), "A displacement-based seismic design method with damage control for RC buildings", *Earthq. Struct.*, **3**(3-4), 413-434.
- Bento, R., Bhatt, C. and Pinho, R. (2010), "Using nonlinear static procedures for seismic assessment of the 3D irregular SPEAR building", *Earthq. Struct.*, **1**(2), 177-195.
- Bracci, J.M., Kunnath, S.K. and Reinhorn, A.M. (1997), "Seismic performance and retrofit evaluation for reinforced concrete structures", *J. Struct. Eng.*, **23**(1), 3-10.
- Chopra, A.K. and Goel, R.K. (1999), "Capacity demand diagram methods based on inelastic design spectrum", *Earthq. Spectra*, **15**(4), 637-656.
- Chopra, A.K. and Goel, R.K. (2002), "A modal pushover analysis procedure for estimating seismic demands for buildings", *Earthq. Eng. Struct. Dyn.*, **31**, 561-582.
- Chopra, A.K. and Chintanapakdee, C. (2004), "Inelastic deformation ratios for design and evaluation of structures: single-degree-of-freedom bilinear systems", *J. Struct. Eng.*, **130**(9), 1309-1319.
- Chopra, A.K. (2008), "Discussion of "observations on the reliability of alternative multiple-mode pushover analysis methods" by T. Tjhin, M. Aschheim, and E. Hernandez-Montes", *J. Struct. Eng.*, **134**(9), 1582-1585.

- Council, B.S.S. (2000), "Prestandard and commentary for the seismic rehabilitation of buildings (FEMA356)", *Federal Emergency Management Agency*, 356, Washington, D.C.
- Fajfar, P. (1999), "Capacity spectrum method based on inelastic demand spectra", *Earthq. Eng. Struct. Dyn.*, **28**(9), 979-993.
- Freeman, S.A. (1978), "Prediction of response of concrete buildings to severe earthquake motion", *Am. Concrete Inst.*, **55**, 589-606.
- Goel, R.K. and Chopra, A.K. (2004), "Evaluation of modal and FEMA pushover analyses: SAC buildings", *Earthq. Spectra*, **20**(1), 225-254.
- Gupta, A. and Krawinkler, H. (1999), "Seismic demands for performance evaluation of steel moment resisting frame structures", Ph.D. Dissertation, Stanford University, CA.
- Gupta, B. and Kunnath, S.K. (2000), "Adaptive spectra-based pushover procedure for seismic evaluation of structures", *Earthq. Spectra*, **16**(2), 367-392.
- Han, S.W. and Chopra, A.K. (2006), "Approximate incremental dynamic analysis using the modal pushover analysis procedure", *Earthq. Eng. Struct. Dyn.*, **35**, 1853-1973.
- Hernández-Montes, E., Kwon, O.S. and Aschheim, M.A. (2004). "An energy-based formulation for firstmode multiple-mode nonlinear static (Pushover) analyses", *J. Earthq. Eng.*, **8**(1), 69-88.
- Krawinkler, H. and Nassar, A.A. (1992). Seismic design based on ductility and cumulative damage demands and capacities. *Nonlinear Seismic Analysis and Design of Reinforced Concrete Buildings*, Eds P. Fajfar and H. Krawinkler. New York: Elsevier Applied Science.
- Krawinkler, H. (1995), "New trends in seismic design methodology", *Proceedings of 10th European Conference on Earthquake Engineering*, Vienna, Austria, September.
- Krawinkler, H. and Seneviratna, G.D.P.K. (1998), "Pros and cons of a pushover analysis of seismic performance evaluation", *Eng. Struct.*, **20**(4-6), 452-464.
- Miranda, E. and Bertero, V.V. (1994), "Evaluation of strength reduction factors for earthquake resistant design", *Earthq. Spectra*, **10**, 357-379
- Miranda, E. (2001), "Estimation of inelastic deformation demands of SDOF systems", *J. Struct. Eng.*, **127**(9), 1005-1012.
- Nassar, A.A. and Krawinkler, H. (1991), *Seismic Demands for SDOF and MDOF Systems*, Report No. 95, John A. Blume Earthquake Engineering Center, Stanford University, CA.
- Newmark, N.M. and Hall, W.J. (1982), "Earthquake Spectra and Design", Berkeley, Calif. Earthquake Engineering Research Inst.
- Prakash, V., Powell, G.H. and Campbell, S. (1993), "DRAIN-2DX base program description and user guide", Report UCB/SEMM-93/17, Department of Civil and Environmental Engineering, University of California at Berkeley, Berkeley, CA.
- Prasanth, T., Ghosh, S. and Collins, K.R. (2008), "Estimation of hysteretic energy demand using concepts of modal pushover analysis", *Earthq. Eng. Struct. Dyn.*, **37**(6), 975-990.
- Ramirez, O.M., Constantinou, M.C., Whittaker, A.S., Kircher, C.A. and Chrysostomou, C.Z. (2002), "Elastic and inelastic seismic response of building with damping systems", *Earthq. Spectra*, **18**(3), 531-547.
- Somerville, P., Punyamurthula, S. and Sun, J. (1997), "Development of ground motion time histories for phase 2 of the FEMA/SAC Steel Project", SAC background documentation, SAC/BD 97-04, Sacramento, CA.
- Vidic, T., Fajfar, P. and Fischinger, M. (1994), "Consistent inelastic design spectra: strength and displacement", *Earthq. Eng. Struct. Dyn.*, **23**(5), 507-521.

Appedix A

To verify the accuracy of C_R equation, the inelastic displacement of SDF systems within a wide period range were calculated under 60 ground motions using C_R equation and $R-\mu-T$ relationship. The results of nonlinear response history analyses were considered as exact answers. Many researchers (Newmark and Hall (1982), Krawinkler and Nassar (1992), Vidic *et al.* (1994), Miranda and Bertero (1994)) also developed equations calculating the inelastic displacement using $R-\mu-T$ relationship. Fig. A.1 shows the inelastic displacements calculated using different procedures. As shown in this figure, the procedure using C_R equation produced inelastic displacements matching those obtained using nonlinear response history analyses compare with other procedures using $R-\mu-T$ relations.

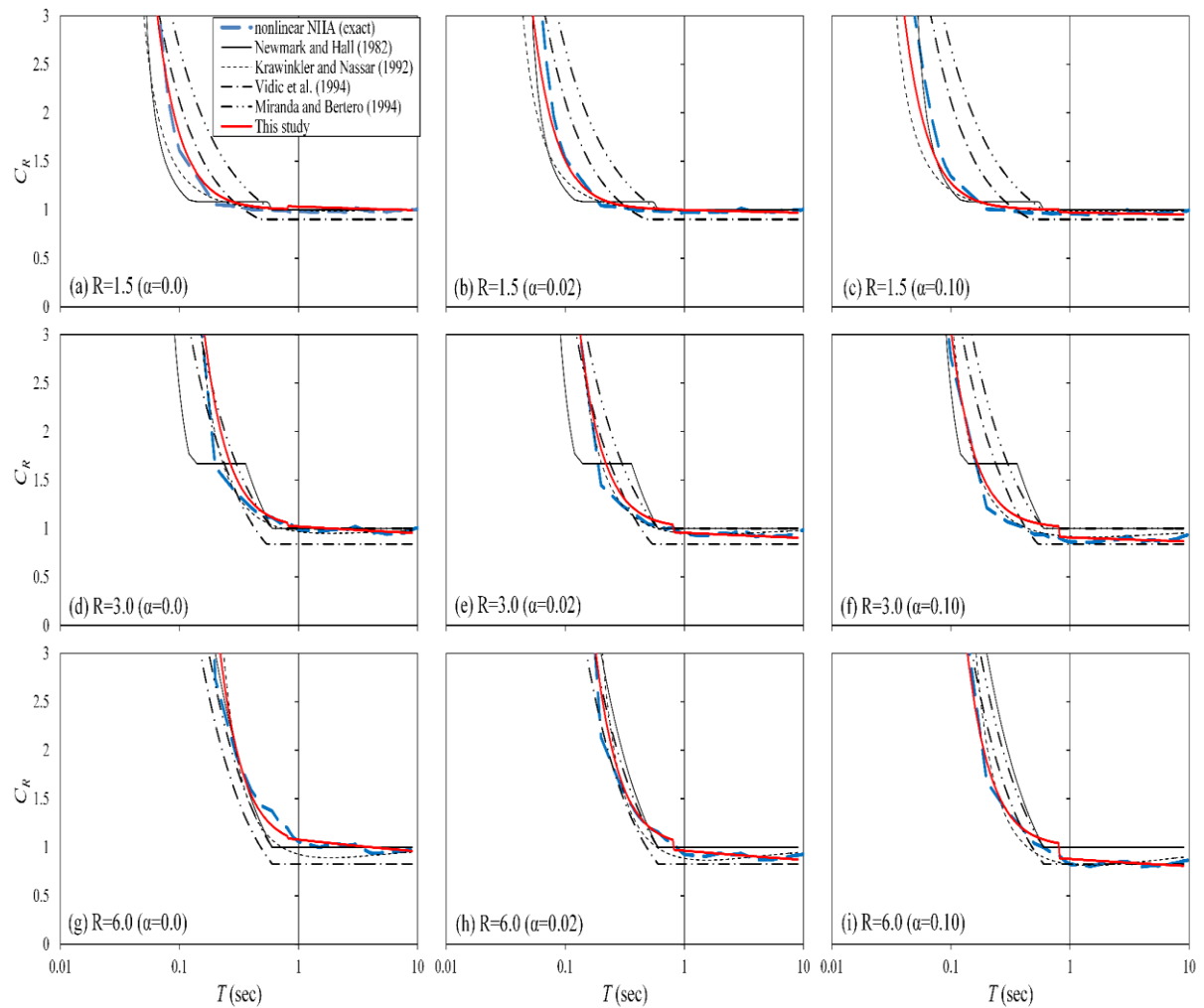


Fig. A.1 Comparison of factor according to factor and of SDF systems